Available online at www.sciencedirect.com
SCIENCE DIRECT®
Journal of Nuclear Materials 352 (2006) 36–41
journal of nuclear materials
www.elsevier.com/locate/jnucmat

In situ creep under helium implantation of titanium–aluminium alloy

J. Chen [a,*], P. Jung [b], M. Nazmy [c], W. Hoffelner [a]

[a] Department of Nuclear Energy and Safety, Paul Scherrer Institut, CH-5232 Villigen PSI, Switzerland
[b] Foschungszentrum Jülich, D-52425 Jülich, Germany
[c] ALSTOM POWER, Haseltrasse, CH-5401 Baden, Switzerland

Abstract

The intermetallic alloy Ti–47Al–2W–0.5Si (at.%) has been homogeneously implanted with $^4He^{2+}$ ions under uniaxial tensile stresses from 20 to 450 MPa to a maximum dose of about 0.16 dpa (1370 appm-He) with displacement damage rates of 2×10^{-6} dpa s^{-1} at temperatures of 573 and 773 K. Strain under implantation was determined by Linear Variable Displacement Transformer (LVDT), while changes of microstructure were investigated after implantation by Transmission Electron Microscopy (TEM). Irradiation creep strain showed a pronounced transient behaviour, virtually independent of temperature, with a stress dependence which can be approximately described by a creep compliance of 8×10^{-6} dpa^{-1} MPa^{-1} up to stresses of 350 MPa. The microstructure of the as-received material consisted of a patch-work of mainly lamellar γ/α_2 colonies and equiaxed γ-grains with islands of precipitates. Only 'black dot' damage was observed after implantation at 573 K under different stresses, while implantation at 773 K yielded a dense population of bubbles and dislocation loops, mostly mutually attached.

PACS: 61.72.Ff; 62.20.Hg

1. Introduction

Recently, concepts for future nuclear fission plants are studied intensively world wide within the framework of the international Generation IV-initiative Forum (GIF) [1]. Among various reactor technologies suggested by the GIF, Very High Temperature Reactors (VHTR) and Gas Cooled Fast Reactors (GFR) are proposed to be studied in the USA and France, respectively. Different to current light water reactors (LWR), VHTR and GFR will operate at much higher temperatures and they will use helium as coolant. The high temperatures (up to 1273 K) not only improve the thermal efficiency but also open new applications of process heat, for instance the production of hydrogen, intending to replace petroleum supplying of clean energy. Reliable high temperature materials are a key issue for successful operation of future VHTR and GFR.

* Corresponding author. Tel.: +41 56 310 2280; fax: +41 56 310 4595.
E-mail address: jiachao.chen@psi.ch (J. Chen).

0022-3115/$ - see front matter © 2006 Elsevier B.V. All rights reserved.
doi:10.1016/j.jnucmat.2006.02.039

Intermetallic alloys, in particular γ-TiAl alloys, have been developed and examined for high temperature applications to replace nickel-based superalloys. They show several advantages compared to nickel-based superalloys: higher elasticity modulus, lower density and better mechanical behaviour at higher temperatures. Moreover, these intermetallic alloys retain a good dimensional stability and, unlike ceramics, they are ductile at elevated temperature. All these features make them very attractive for high temperature applications. Recently, ductility of γ-TiAl alloys at room temperature has been improved steadily by alloy design efforts, including microstructural modification by thermomechanical treatments. For instance, at ALSTOM Power (formerly ABB) a proprietary γ-TiAl alloy named ABB2-TiAl alloy (Ti–46Al–2W–0.5Si, at.%) has been developed [2,3]. The material shows reasonable ductility at room temperature and strength of 600 MPa is maintained at least up to 1173 K.

Titanium aluminides are not only interesting for application in advanced nuclear power plants because of their high temperature strength, but also show lower neutron-induced radioactivity in comparison to stainless steels in fission environments [4]. Investigations on irradiation effects in γ-TiAl based alloys have been carried out [5–11], mainly focusing on microstructural changes after He-implantation [6], e^--irradiation [7,8], n-irradiation [9], and heavy ion irradiation [10,11]. But only few data exist on mechanical properties of irradiated γ-TiAl alloys. One experiment showed that instead of the usual irradiation embrittlement, the ductility of a γ-TiAl alloy astonishingly increased after neutron irradiation [5], indicating good potential in nuclear fission environments. Apparently no data are available on creep properties of γ-TiAl alloys during irradiation or He-implantation. However, such information is required for an assessment of the potential use of these materials in advanced nuclear power plants. Therefore, in the present work, in situ irradiation creep of a γ-TiAl alloy under He-implantation and its influence on microstructure was investigated.

2. Experimental

A γ-TiAl based intermetallic alloy supplied by ALSTOM POWER was used in this study. Its composition is given in Table 1. The miniaturized dog-bone shaped samples were cut by spark-erosion from the bulk, then sliced to 0.3 mm thickness and finally mechanically polished from both sides to 0.2 mm. The final sample had an overall size of 28 mm in length, 8 mm in width and 0.2 mm in thickness, with a gauge volume of $10 \times 2 \times 0.2$ mm^3.

He-implantation was performed at the Compact Cyclotron of Forschungszentrum Juelich. Details of the experimental set-up are described in Refs. [12,13]. With 24 MeV $^4He^{2+}$ ions passing through a magnet scanning system and a degrader wheel with 24 Al-foils of variable thicknesses, the 0.2 mm thick samples were homogeneously implanted under uniaxial stress. Typical implantation rates were 0.02 appm (atom parts per million) per second. The concurrent production of displacement damage was calculated by TRIM and SRIM [14,15] for a displacement threshold energy of 40 eV and a binding energy of 2 eV, giving per implanted He-atom 128 displacements on the front side and 70 on the back side, averaging to 117 displacements per He-ion. From this a displacement rate of about 2.3×10^{-6} dpa (displacements per atom) per second is derived. The irradiation creep strains were monitored by LVDT (Linear Variable Displacement Transformer) during beam-off periods, and implantation at constant applied stress was continued until the strain rate became constant (stationary creep). Then the implantation was continued on the same specimen at a different stress in the range from 20 to 450 MPa. During each run, temperature was fixed (573 or 773 K). Two specimens were tested at each of both temperatures. The temperature distribution along the gauge region was monitored by an infrared pyrometer.

In order to save materials and reduce radioactivity, 1 mm diameter discs were prepared for transmission electron microscopy (TEM). Firstly, 1 mm discs were punched out from the 200 μm thick creep specimens and glued into a 1 mm hole in a disc of 3 mm in diameter and 200 μm in thickness.

Table 1
Chemical composition (wt%)

Element	Ti	Al	W	Si	Fe	O	H	N
wt%	Balance	30.62	9.00	0.32	0.044	0.077	0.002	0.009
at.%	Balance	46.11	2.02	0.48	0.017	0.168	0.040	0.093

Afterwards this assembly was mechanically polished from both sides down to 0.1 mm thickness, and finally was electrochemically polished in a Tenupol-3 with a solution of 5 vol.% perchloric acid (60%) and 95 vol.% methanol at a temperature of 268 K and a current of 150 mA . TEM examinations were performed with a JEM 2010 at PSI.

3. Results and discussion

Figs. 1 and 2 show the plastic strain $\varepsilon(\sigma) = \frac{\Delta l}{l_0}$ of the γ-TiAl alloys for a stress σ during implantation/irradiation as a function of displacement dose at 573 and 773 K, respectively. The two specimens in Fig. 1 were implanted at 573 K at consecutive stresses of 200, 100 and 350 MPa, and of 20 and 350 MPa, respectively. Both sets of data show a long-lasting transient stage before stationary creep is reached. The test at 350 MPa in the first run did not reach a constant rate due to premature failure in the clamp head. Irradiation induced strain rates described by irradiation-creep rates, ε', i.e., strain rate/damage-dose rate (in unit of dpa^{-1}) were obtained from the straight lines in Figs. 1 and 2. The contribution of transient strains, which are tentatively ascribed to dimensional changes induced by collected point defects and their clusters, were subtracted at a given dose yielding the corrected value ε'_c as follows:

$$\varepsilon'_c(\sigma) = [\varepsilon'(\sigma) - \varepsilon'(\sigma_1)] \cdot \frac{\sigma}{\sigma - \sigma_1}, \quad (1)$$

where $\varepsilon'(\sigma)$ is irradiation-creep rate measured at stresses (σ) in the range of 100–450 MPa with baseline of $\sigma_1 = 20$ MPa. Measurements at lower stresses were not possible at sufficient precision. These corrected values (ε'_c) are plotted in Fig. 3 as a function of applied stress for both implantation temperatures. The data can be fitted by a linear stress dependence at least up to 350 MPa (solid line):

$$\varepsilon'_c(\sigma) = \zeta \cdot \sigma \quad \text{with}$$
$$\zeta = 8 \times 10^{-6}\ \mathrm{dpa}^{-1}\ \mathrm{MPa}^{-1} \text{ for } \sigma \leqslant 350\ \mathrm{MPa}, \quad (2)$$

or approximately by an overall quadratic dependence (dashed line):

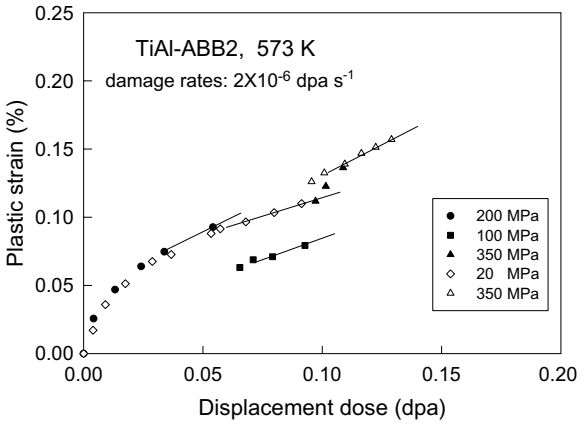

Fig. 1. Plastic strain of two TiAl alloy specimens (open and filled symbols, respectively) during He-implantation at 573 K as a function of displacement dose at given stresses.

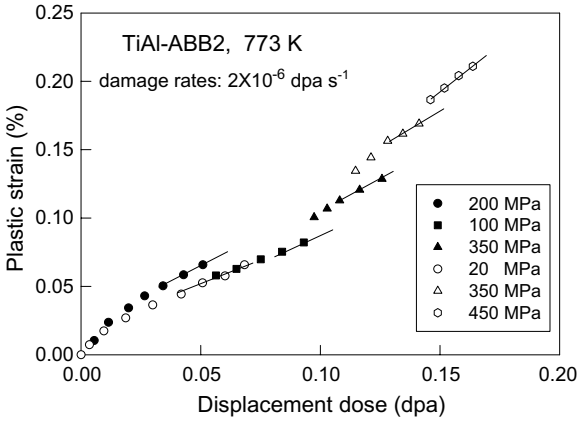

Fig. 2. Plastic strain of two TiAl alloy specimens (open and filled symbols, respectively) during He-implantation at 773 K as a function of displacement dose at given stresses.

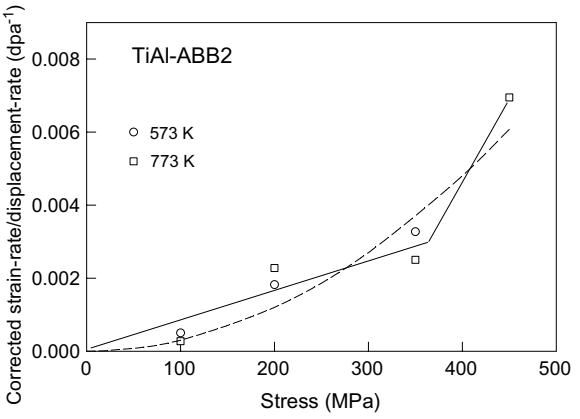

Fig. 3. Corrected irradiation creep rates per displacement rates of TiAl as a function of tensile stress under He-implantation at 573 and 773 K. Solid and dashed lines are linear and quadratic fit, respectively.

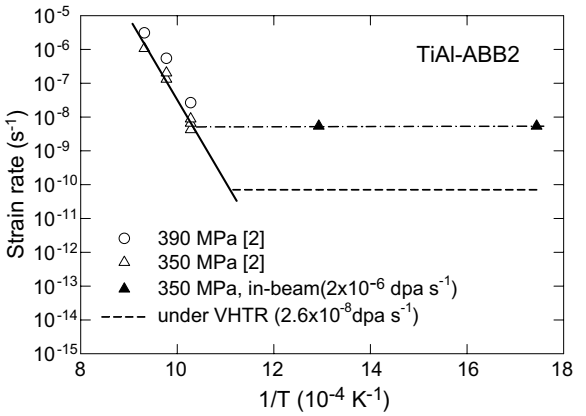

Fig. 4. Temperature dependence of creep rates of TiAl without irradiation (solid line) and under He-implantation (dash-dotted) and expected VHTR conditions (dashed line).

$$\varepsilon_c'(\sigma) = \xi \cdot \sigma^2 \quad \text{with} \quad \xi = 3 \times 10^{-8}\ \text{dpa}^{-1}\ \text{MPa}^{-2}. \tag{3}$$

This behaviour is similar to pure metals [15], nickel-based alloys and austenitic stainless steels [17]. A creep compliance, i.e., creep rate per dose rate and stress can be determined to be $8 \times 10^{-6}\,\text{dpa}^{-1}\,\text{MPa}^{-1}$ from Eq. (2).

The temperature-dependence of strain rates with and without He-implantation is given in Fig. 4. Expected creep rates under conditions expected for future VHTR conditions are included. The present data show that the irradiation creep rate of γ-TiAl alloy is the same for 573 K and for 773 K. Extrapolation of irradiation data at 350 MPa matches the thermal creep line at 973 K and 900 K for the present He-implantation and under VHTR condition, respectively. According to earlier experimental findings [16–18] and theoretical understanding [19,20], irradiation creep dominates at low temperatures when thermal vacancy concentration is negligible. Only a minor temperature dependence is expected in this area. When thermal creep starts at high temperature it will prevail and irradiation will have no major influence on creep rates except eventually via irradiation induced microstructural or compositional changes.

Microstructures of γ-TiAl alloy in the as-received condition, and implanted under stresses at 573 K, and at 773 K are shown in Figs. 5–7. The original material showed lamellar structures, consisting mainly of γ/α_2 patch-work (Fig. 5, left) and equiaxed γ-grains with islands of precipitates (Fig. 5, right). The detailed microstructure in the as-received materials can be seen also in Ref. [3]. After implantation at 573 K the γ-phase shows no bubbles, but only a few 'black dots' with a size of about 3 nm (Fig. 6, right). However, the specimen implanted at 773 K shows a dense population of spherical bubbles with a diameter of 2 nm (Fig. 7, left) and loops of a typically 9 nm diameter (Fig. 7, right). Mostly bubbles and loops are attached to each other.

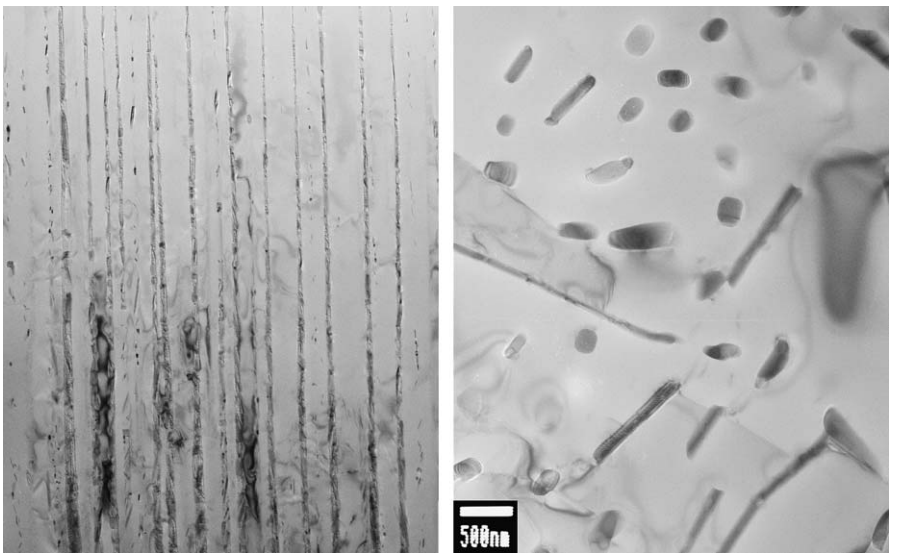

Fig. 5. Microstructure of as received TiAl alloy. The left image shows the lamellar structure of γ/α_2 mixtures (γ bright), the right image shows equiaxed grains with islands of precipitates.

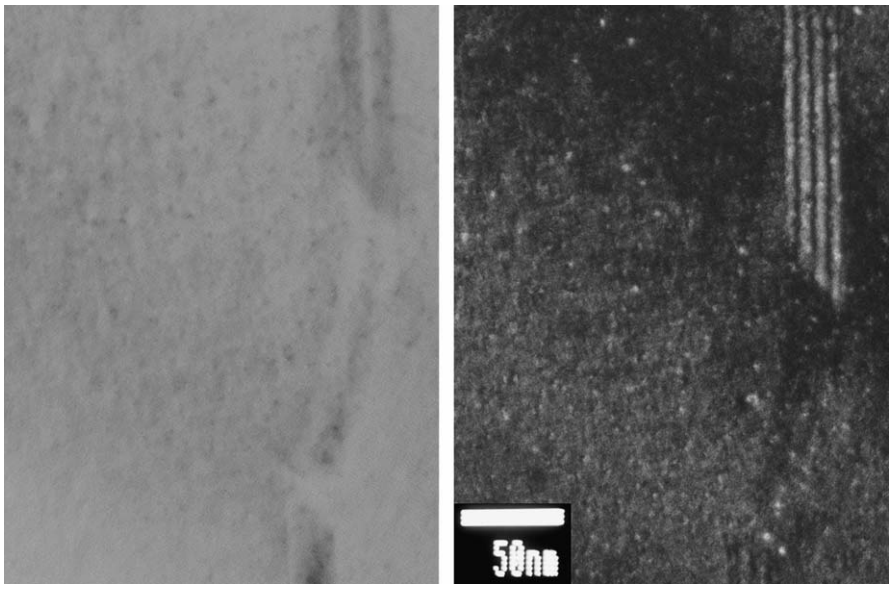

Fig. 6. Microstructure of TiAl alloy after He-implantation under different stresses at 573 K up to 0.11 dpa. Under-focal bright-field imaging (left) demonstrates the absence of bubble formation, while weak-beam dark-field imaging (WBDF, right) shows some 'black dot' damage. Zone is close to [101] with $g = (020)$.

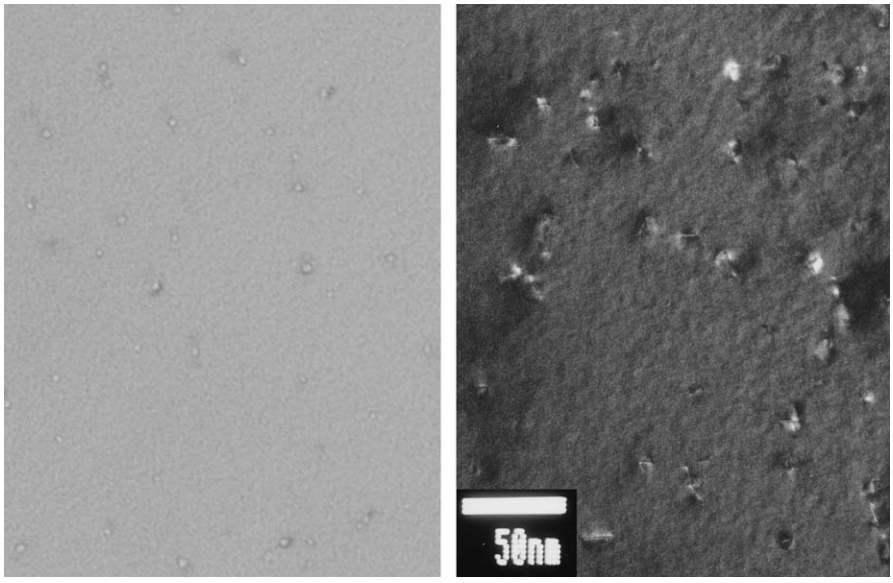

Fig. 7. Microstructure of TiAl alloy after He-implantation under different stress at 773 K up to 0.13 dpa. Under-focal bright-field imaging (left) demonstrates bubble formation, while WBDF imaging (right) shows dislocation loops with habit planes of {111}. Zone close to [101] with $g = (020)$.

Estimated relative volume change by bubble formation is 6.8×10^{-5} which gives a negligible contribution to the measured length change. In all cases, very few dislocations were observed. The loops have habit planes of {111}, in agreement with earlier results after He-implantation without external stress [6]. There is no evidence for a dependence of loop growth on orientation with respect to stress direction. But this point needs further investigation by more sophisticated experiments.

4. Conclusions

In situ creep experiments under helium implantation were performed at 573 and 773 K on a γ-TiAl intermetallic alloy up to displacement doses of 0.16 dpa (1370 appm helium). Subsequently, the changes of microstructures were investigated by TEM.

Based on the present results the following conclusions can be drawn:

(1) Creep rate per displacement rate can be fitted by a linear stress dependence up to 350 MPa, while above 350 MPa the stress dependence increases.
(2) From this fit a creep compliance, i.e., creep rate per dose rate and stress, of 8×10^{-6} dpa^{-1} MPa^{-1} is derived for both temperatures of 573 and 773 K.
(3) From the present results, it is expected that thermal creep will be the dominant deformation process in future VHTRs where helium production can be neglected.
(4) The sample which was He-implanted at 573 K under stress shows 'black dots' with a size of ~3 nm. Bubbles (~2 nm) and loops (~9 nm) were formed in the sample He-implanted at 773 K under stresses. The loops have habit planes of {1 1 1}.

Acknowledgements

The authors would like to thank H. Ullmaier for valuable discussions.

References

[1] A Technology Roadmap for Generation IV Nuclear Energy System, Issued by the US DOE Nuclear Energy Research Advisory Committee and the Generation IV International Forum, GIF-002-00, December 2002.
[2] M. Nazmy, M. Staubli, US Patent 5,207,982 & EP. 45505 B1.
[3] J. Lapin, M. Nazmy, Mater. Sci. Eng. A380 (2004) 298.
[4] S. Mori, H. Miura, S. Yamazaki, T. Suzuki, A. Shimizu, Y. Seki, T. Kunugi, S. Nishio, N. Fujisawa, A. Hishinuma, M. Kikuchi, Fus. Technol. 21 (1993) 1744.
[5] A. Hishinuma, M. Tabuchi, T. Sawai, K. Nakata, Phys. Stat. Sol. (a) 167 (1998) 521.
[6] K. Nakata, K. Fukai, A. Hishinuma, K. Ameyama, M. Tokizane, J. Nucl. Mater. 202 (1993) 39.
[7] R. Wuerschum, K. Badura-Gergen, E.A. Kuemmerle, C. Grupp, H.E. Schaefer, Phys. Rev. B54 (1996) 849.
[8] G. Sattonnay, C. Dimitrov, C. Corbel, O. Dimitrov, Intermetallics 7 (1999) 23.
[9] Y. Miwa, T. Sawai, K. Fufai, D.T. Hoelzer, A. Hishinuma, J. Nucl. Mater. 283–287 (2000) 273.
[10] A.T. Motta, J. Nucl. Mater. 244 (1997) 227.
[11] M. Song, K. Mitsuishi, M. Takeguchi, K. Furuya, T. Tanabe, T. Noda, J. Nucl. Mater. 307–311 (2002) 971.
[12] P. Jung, A. Schwarz, H.K. Sahu, Nucl. Instr. and Meth. A 234 (1985) 331.
[13] H. Schroeder, P. Batfalsky, J. Nucl. Mater. 103&104 (1981) 839.
[14] J.P. Biersack, L.G. Haggmark, Nucl. Instr. and Meth. 174 (1980) 93.
[15] J.F. Ziegler, J.P. Biersack, U. Littmark, The Stopping and Range of Ions in Solids, Pergamon, New York, 1985.
[16] P. Jung, M.I. Ansari, J. Nucl. Mater. 138 (1986) 40.
[17] P. Jung, J. Nucl. Mater. 113 (1983) 133.
[18] P. Jung, C. Schwaiger, H. Ullmaier, J. Nucl. Mater. 85 (1979) 867.
[19] H. Ullmaier, W. Schilling, Radiation Damage in Metallic Reactor Materials in 'Physics of Modern Materials', vol. 1, International Atomic Energy Agency, Vienna, 1980, p. 301.
[20] L.K. Mansur, in: G.R. Freemann (Ed.), Kinetics of Nonhomogeneous Processes, Wiley-Interscience, New York, 1987.